

A Risk Estimation Method for Airborne Infectious Diseases Based on Aerosol Transmission in Indoor Environment

Zhuyang Han, Wenguo Weng, Quanyi Huang, and Shaobo Zhong

Abstract—Airborne transmission of respiratory infectious disease in large indoor environment can cause outbreaks of infectious diseases, which may lead to many infection cases and significantly influence the public health. This work investigated the aerosol transmission and risk distribution characteristics in larger indoor environment. Eulerian-Lagrangian approach was adopted for the aerosol dynamics simulation. The aerosol transmission is numerical simulated under natural ventilation and air-condition ventilation, and the effects of inlet velocity, aerosol release location and multiple sources are also studied. The infection risk distribution is assessed by using the dose-response model. A risk estimation method for airborne infectious diseases is also proposed based on the distribution characteristics of the infection risk. The infection risk distribution in indoor environment can be approximately estimated according to the average airflow velocity in the environment. This method can be used for the risk evaluation of larger indoor environment, in which accurately calculation and simulation of aerosol transmission is computationally expensive and infeasible.

Index Terms—aerosol dispersion, aerodynamic effects, risk assessment, indoor air

I. INTRODUCTION

Nowadays, respiratory infectious diseases are threatening the life of humans around the world [1]. In the past four decades, airborne transmission of respiratory infectious diseases within enclosed environment has been widely reported by many epidemiology reports [2-5]. According to the transmission mechanism of respiratory infectious disease, the diffusion and dispersion of the aerosols expelled by

respiratory activities are important and necessary for infection risk assessment [6]. Airborne transmission of respiratory infectious disease in large indoor environment (e.g. large workshop, factory premise, conference room, and convention and exhibition center) may cause outbreaks of infectious diseases. Due to the poor protective measures in these large enclosed area, outbreaks of airborne diseases may lead to many infection cases and significantly influences the public health.

This work focus on the transmission of respiratory infectious diseases in large indoor environment. The airborne transmission of the aerosols were numerical simulated. The infection risk distribution in the area was quantitatively evaluated, and a risk estimation method was proposed based on the risk assessment results. The numerical approach was given in Section 2. The characteristics of risk distribution and the risk estimation method were demonstrated in Section 3, followed by the conclusions.

II. METHODS

A. Numerical domain

In this work, the numerical domain was set as a large indoor factory premise. Two types of ventilation systems were numerical investigated: natural ventilation and air-condition ventilation, as shown in Fig. 1. For natural ventilation environment, the size of the numerical domain was $100\text{m} \times 30\text{m} \times 5\text{m}$, large enough for the simulation of aerosol transmission. No central air conditioning or distributed ventilation facility was used. Natural ventilation was used for the whole area. The ventilation airflow came into the area from surface ABCD, and the airflow direction was from surface ABCD to EFGH. In this CFD domain, indoor facilities were also numerical set to represent the lathes, assembly line or other facilities used in large factory premise, as shown in Fig. 1 (a). The origin of coordinate system was located at point D. The two surfaces of the cabin (ADHE and BCGF) were set as periodic boundary so that the domain could unlimited expansion in Y direction. For air-condition ventilation environment, the size of the numerical domain was $50\text{m} \times 60\text{m} \times 5\text{m}$. The ventilation system located on the ceiling of the domain. The ventilation airflow came into the area from surface ABFE, and the direction of the airflow was from surface ABFE to DCGH. Indoor facilities were also numerical set, as shown in Fig. 1 (b). The origin of coordinate system was located at point D. The two couples of surfaces (ADHE and BCGF, and ADCB and EHGf) were set as

Manuscript received Mar 12, 2014; revised Apr 8, 2014. This work was supported in part by the National Natural Science Foundation of China (Grant No. 51076073, 91024018 and 91224004), China National Key Basic Research Special Funds Project (Grant No. 2012CB719705), and Tsinghua University Initiative Scientific Research Program (Grant No. 2012THZ02160).

Zhuyang Han is with the Institute of Public Safety Research, Department of Engineering Physics, Tsinghua University, Beijing, 100084, China (e-mail: hanzhuyang@gmail.com).

Wenguo Weng is with the Institute of Public Safety Research, Department of Engineering Physics, Tsinghua University, Beijing, 100084, China. (phone: +86-10-62792894; fax: +86-10-62792863; e-mail: wgweng@tsinghua.edu.cn).

Quanyi Huang is with the Institute of Public Safety Research, Department of Engineering Physics, Tsinghua University, Beijing, 100084, China.. (e-mail: qyhuang@tsinghua.edu.cn).

Shaobo Zhong is with the Institute of Public Safety Research, Department of Engineering Physics, Tsinghua University, Beijing, 100084, China. (e-mail: zhongshaobo@tsinghua.edu.cn).

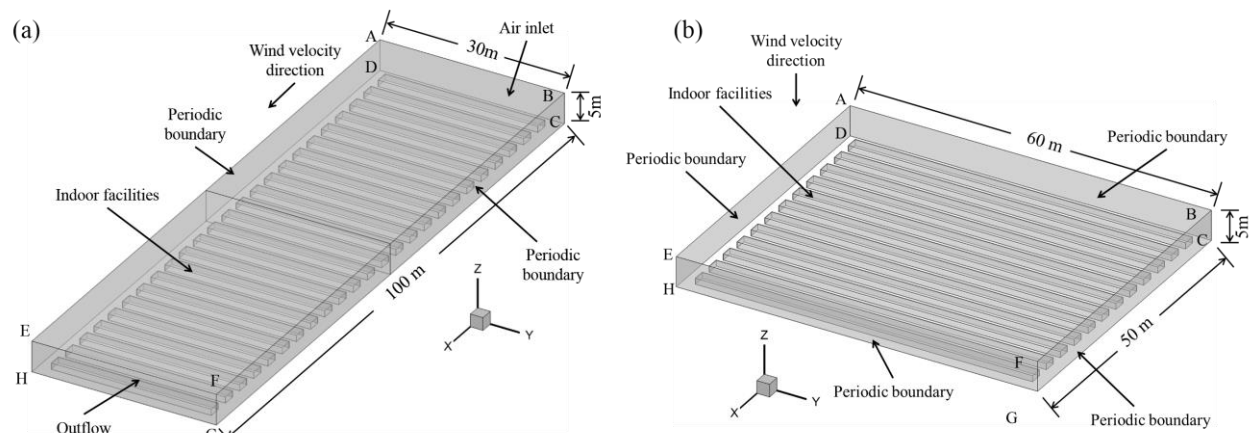


Fig. 1. Layout of the two ventilation environment. (a) natural ventilation, (b) air-condition ventilation.

periodic boundary, respectively. So this domain could also unlimited expansion, both in X and Y direction. Gambit (version 2.4.6) was used to build the geometry domain and generate the cells for numerical simulation. The whole region was meshed by structured grids of hexahedron. The maximum mesh size was 0.2m, and the total number of the grids was 1,681,500 for natural ventilation environment and 1,424,500 for air-condition ventilation environment.

B. Aerosol transmission simulation

To simulate the transmission of the aerosols in large indoor environment, the Computational Fluid Dynamics (CFD) software ANSYS (version 12.1.4) was utilized in this study. The Eulerian-Lagrangian approach was adopted for the aerosol dynamics simulation in enclosed environments. This method has been widely used for the numerical simulation of aerosol transmission in indoor environment [7-10]. In this approach, the governing equations of the carrier phase were numerically solved in the computational geometry based on the Eulerian framework [7]. The governing equations of the discrete phase were described in the Lagrangian framework. Each aerosol released from the injection point was tracked individually in the Lagrangian frame for its instantaneous position and velocity. In the transient simulation, the interaction between the discrete phase and the continuous phase was also considered and computed during the continuous phase iterations. The particles were tracked using the Lagrangian method along with the flow equations at the end of each time step. The Re-Normalization Group (RNG) k- ϵ model was adopted to simulate the turbulent flow [11, 12]. An enhanced two-layer wall treatment was employed for the prediction of aerosol deposition [8]. Wall unit adaptation was applied in wall-adjacent cells when creating the meshes to ensure that the values of the wall unit y^+ meet the requirements of the enhanced wall treatment [9].

In this work, the droplets expelled by cough of the index patient were used as the infectious aerosols of influenza for numerical simulation and risk assessment. According to experimental measurements of cough droplets, the quantity of the droplets smaller than $3\mu\text{m}$ was quite small, and the droplets larger than $100\mu\text{m}$ might fall down to the ground immediately after they were expelled [13, 14]. So in this work, the original size range of the aerosols was $3\mu\text{m}\sim 112\mu\text{m}$ and ten size classes were used to simulate the size distribution. Considering that the equilibrium diameter after evaporation

was 50% of the original size [15], the size range of the aerosol injections was $1.5\sim 56\mu\text{m}$ and the size distribution followed the experimental results given by Duguid (1946).

The boundary conditions of the numerical simulation are shown in Table I. The airflow pattern in the two numerical domains was first simulated in steady-state. The investigated cases are given in Table II. Cases 1~10 were used to simulated the aerosol transmission in the two environments under five different inlet velocity, including 0.1m/s, 0.2m/s, 0.3m/s, 0.4m/s, and 0.5m/s. This range of air inlet velocity was used to simulate normal indoor environment which was quite common in labor-intensive factories in East and Southeast Asia. Cases 11~14 were used to comparing the influence of aerosol release location on the affected region. Cases 15~17 were used to simulate the cases that multiple sources exited in the numerical domain. Each case was computed in a 4-node Linux cluster. Each node of the cluster had eight processors (2.4 GHz Intel 64) and 16 GB of memory.

TABLE I
THE BOUNDARY CONDITIONS IN THE NUMERICAL SIMULATION

Surface	Velocity	Temperature	Discrete phase
Ceiling	No slip	297K	Trap
Side wall (natural ventilation)	No slip	293K	Trap
Floor	No slip	291K	Trap
Indoor facilities	No slip	Adiabatic	Trap
Outlet	Outflow		Escape
Side surface	Periodic boundary		Escape

TABLE II
THE CASES INVESTIGATED IN THE NUMERICAL SIMULATION

Case No.	Ventilation	Inlet velocity	Aerosol release location
case 1	Natural	0.1	(9, 15, 1.5)
case 2	Natural	0.2	(9, 15, 1.5)
case 3	Natural	0.3	(9, 15, 1.5)
case 4	Natural	0.4	(9, 15, 1.5)
case 5	Natural	0.5	(9, 15, 1.5)
case 6	Air-condition	0.1	(25, 25, 1.5)
case 7	Air-condition	0.2	(25, 25, 1.5)
case 8	Air-condition	0.3	(25, 25, 1.5)
case 9	Air-condition	0.4	(25, 25, 1.5)
case 10	Air-condition	0.5	(25, 25, 1.5)
case 11	Natural	0.3	(2, 15, 1.5)
case 12	Natural	0.3	(25, 15, 1.5)
case 13	Natural	0.3	(50, 15, 1.5)
case 14	Natural	0.3	(75, 15, 1.5)
case 15	Natural	0.3	(25, 15, 1.5)
case 16	Natural	0.3	(9, 15, 1.5) and (25, 15, 1.5)
case 17	Air-condition	0.3	(25, 25, 1.5) and (25, 15, 1.5)

C. Risk assessment

Based on the numerical simulation results, the infection risk distribution was investigated by using the dose-response model in the risk assessment [16]. The exposure levels of the occupants were assessed according to the concept of intake fraction [6, 17], which demonstrated the fraction of the quantity of pathogens deposited on the target infection site in the respiratory tract to the total quantity of pathogens produced by the index patient [18]:

$$D(x, t) = \frac{\sum_{l=1}^m \beta_l c p \int v(x, t)_l h_l f(t) dt}{N_c} \quad (1)$$

where $D(x, t)$ is the intake fraction of the susceptible occupants for one cough. x is the spatial location. c is the pathogen concentration in the expiratory fluid, 10^5 pfu/ml for influenza [19]. p is the pulmonary ventilation rate, 7.5l/min [6]. $f(t)$ is the viability function of pathogens in the aerosols, 75% after aerosolization and 2% additional decrease per minutes [18]. m is the total number of size bins. N_c is the total quantity of pathogens produced in a cough, $N_c = V_c c$, where V_c is the total volume of the droplets produced in a cough, 6.7×10^{-3} ml [6, 20]. h_l is the ratio of the number of droplets of the l th size bin in a cough to the number of injected particles in the numerical model, in which the number of droplets of the l th size bin can be calculated according to the original size distribution of the cough and V_c . $v(x, t)$ is the volume density of expiratory droplets, ml/l of air. β_l is

the respiratory deposition fraction of the aerosols of the l th size bin, %, which can be calculated according to the size and deposition location of the aerosols, head airway and tracheobronchial regions for influenza [21].

It was tedious and time-consuming to model every cough during the exposure time interval to obtain $v(x, t)$ at different locations. Considering other aerodynamic size-dependent factors, a stochastic non-threshold dose-response model for airborne pathogens can be formed [18]:

$$P_l(x, t_0) = 1 - \exp\left(-\sum_{l=1}^m r_l \beta_l f_s t_0 c p \int_0^{t_0} v(x, t)_l h_l f(t) dt\right) \quad (2)$$

$$= 1 - \exp(-r N_c f_s t_0 D(x, t_0))$$

where P_l is the infection risk distribution; t_0 is the exposure time interval, 8hr for this study; f_s is the cough frequency, 18/hr [22]; r_l is the infectivity of pathogens in the droplets of the l th size bin; and r is the integrated infectivity factor for all pathogens [18].

III. RESULTS AND DISCUSSION

A. Infection risk distribution

By using the CFD method and the dose-response model, the infection risk distribution in the numerical domain can be obtained. Fig. 2 demonstrates and compares the infection risk distribution in the two numerical domain for cases 1, 3, 5, 6 and 10. As shown in Fig. 2, the airflow motion in these indoor environment significantly influences the transmission of the aerosols. After released, the aerosols will keep on moving

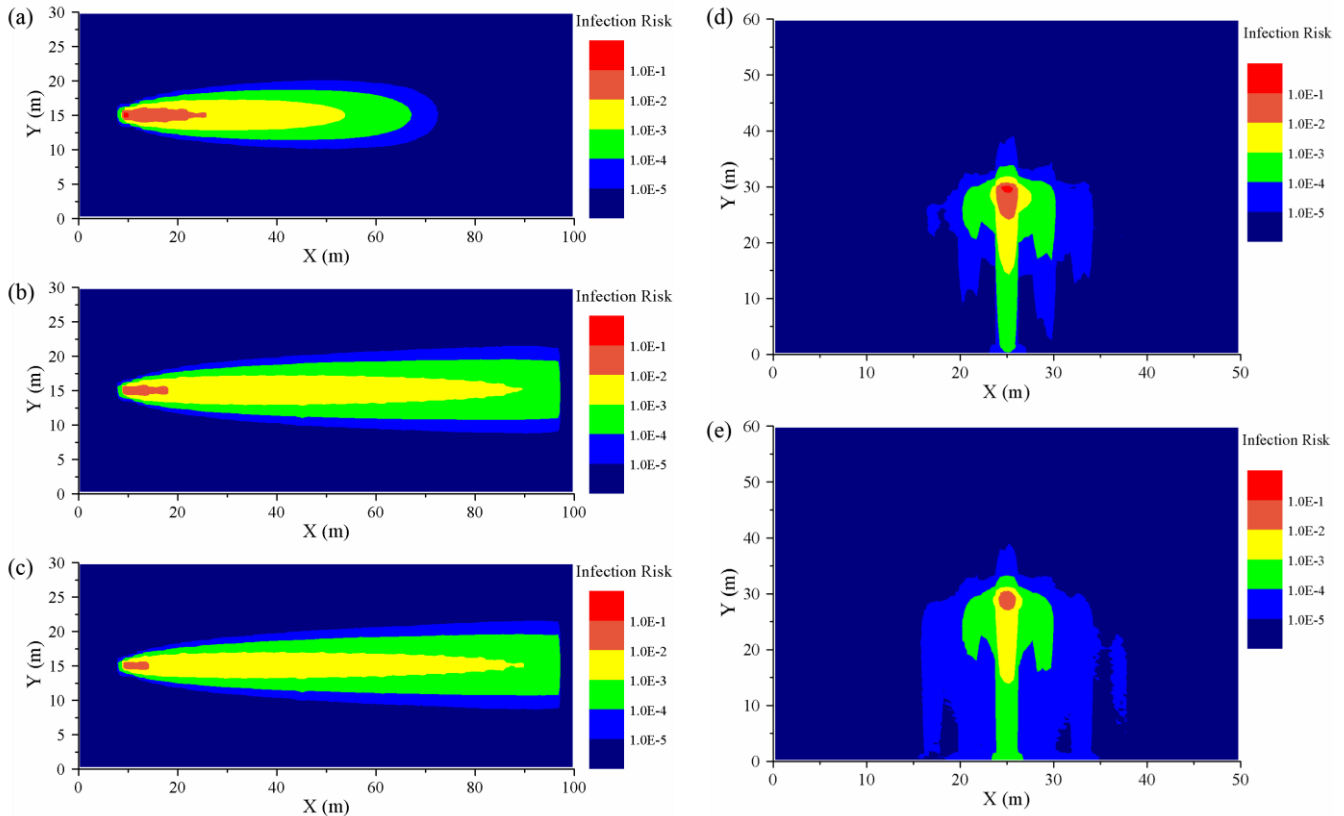


Fig. 2. Risk distribution of natural ventilation and air-condition ventilation environment. (a) case 1, (b) case 3, (c) case 5, (d) case 6, (e) case 10.

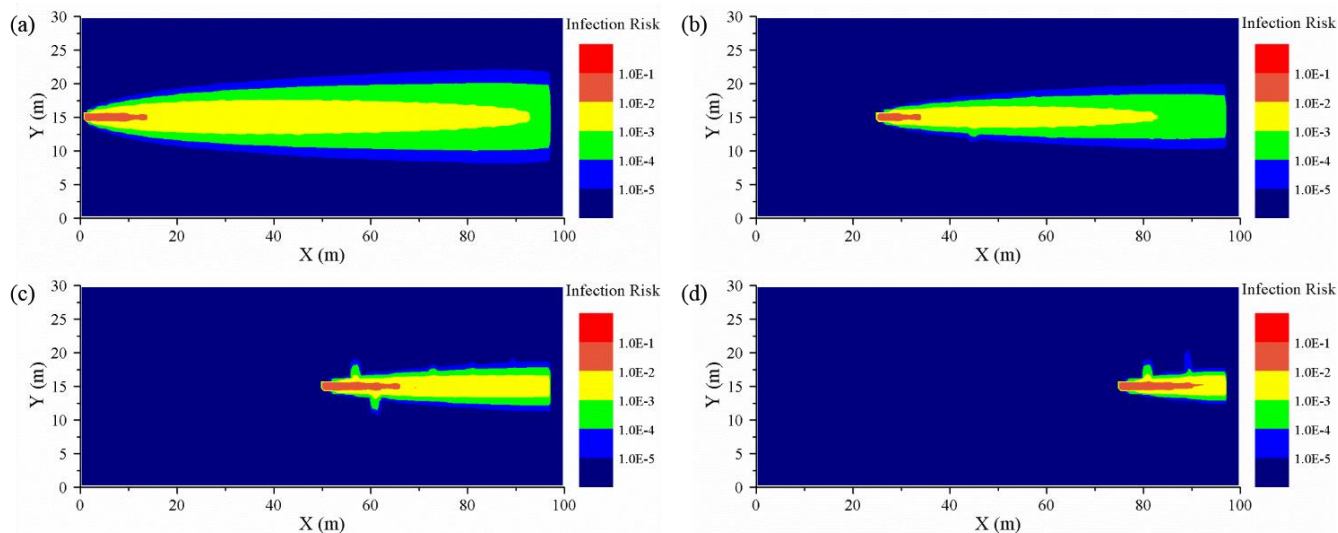


Fig. 3. Risk distribution when the location of aerosol release source is different. (a) case 11, (b) case 12, (c) case 13, (d) case 14.

towards the outlet surface, following the direction of the indoor airflow. So the airborne transmission of the aerosols is highly depended on the indoor airflow motion. Larger airflow velocity may promote the transmission of the aerosols and lead to a larger affected region.

To demonstrate the effects of aerosol release location on the affected region, Fig. 3 shows the risk distribution of cases 11~14. Along the air flow direction (X direction), the affected region covers the whole area from the aerosol release location to the outlet. Since the aerosols are transported by the indoor airflow, the aerosols cannot move towards the inlet surface. So the affected region of the released aerosols is decided by the location of the aerosol source and the airflow motion in the indoor environment. Comparing Fig. 3 and Fig. 2 (a)~(c), it can be seen that the location of aerosol source will not change the distribution characteristics of the infection risk.

Fig. 4 compares the risk distribution when multiple aerosol sources exited in the environment. Fig. 4 (a) and (c) is the risk

distribution when two aerosol sources exited in the area. When each aerosol source exits individually, the aerosol concentration can also be numerical simulated. In Fig. 4 (b) and (d), the risk distribution is calculated by adding the aerosol concentration induced by each aerosol source, and then calculated the intake fraction and infection risk by using equation (1) and (2). By comparing Fig. 4 (a), (b) and (c), (d), it can be seen that the risk distribution is quite similar. So, if a few of aerosol sources exits in the environment, the aerosol concentration can be calculated by adding the aerosol concentration of each individual aerosol source. Then the risk distribution can also be approximately calculated.

To demonstrate the characteristics of the risk distribution of natural ventilation and air-condition ventilation environment, Fig. 5 shows the average infection risk in the affected region and the area of the affected region, respectively. It shows that the average risk decreases quickly with the increase of the inlet velocity. Larger inlet velocity

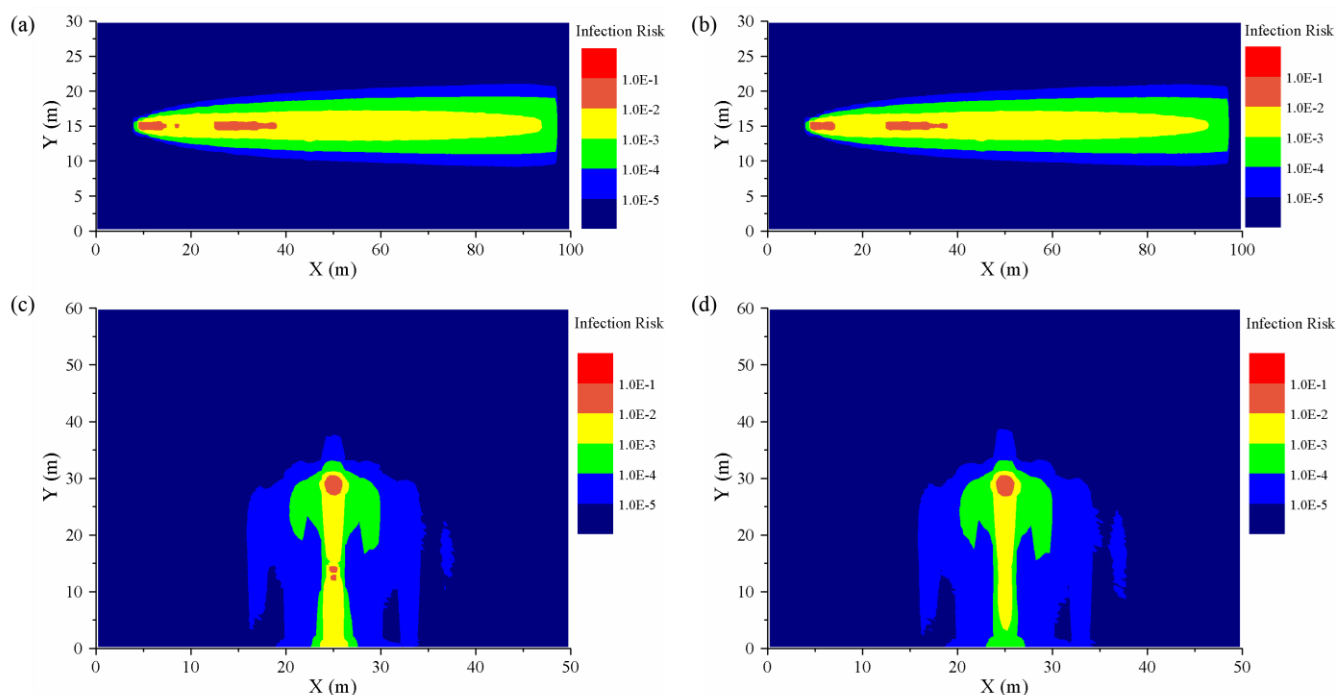


Fig. 4. Risk distribution when multiple aerosol release sources exited in the environment. (a) case 16, (b) case 17, (c) case 3 add case 12, (d) case 8 add case 12.

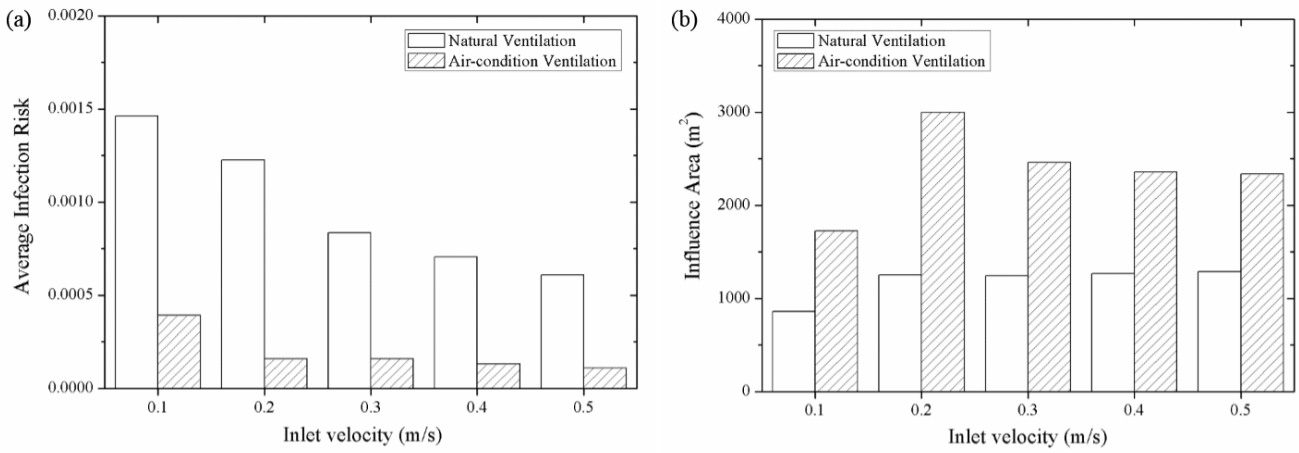


Fig. 5. Characteristics of risk distribution in the two environment. (a) average infection risk, (b) area of affected region.

will lead to a lower aerosol concentration and a smaller average risk. Fig. 5 also indicates that indoor cabin that using air-condition ventilation will have a significantly smaller average infection risk, although the area of affected region is larger. From Fig. 5, it can be concluded that using air-condition ventilation with large inlet velocity will significantly lower the infection risk in indoor environment.

B. A risk estimation method

Fig. 6 shows the risk distribution in Y direction in the natural ventilation environment. It is indicated that the distribution characteristics obviously meet the distribution characteristics of normal distribution. So the risk distribution in Y direction can be quantitatively represented by the normal distribution function, as follows:

$$P(x, y) = A(x) \left(\frac{1}{\sqrt{2\pi}\sigma(x)} \right) e^{-\frac{(y-Y_0)^2}{2\sigma^2(x)}} \quad (3)$$

where $R(x, y)$ is the infection risk at (x, y) ; The aerosol release location is (X_0, Y_0) . $\sigma(x)$ and $A(x)$ are the characteristic parameters of the normal distribution, for variance and coefficient, respectively. The value of these characteristic parameters is related to the location in X direction. In this study, a nonlinear least-square curve fitting analysis is performed to obtain the optimum values of the characteristic parameters required to define the normal

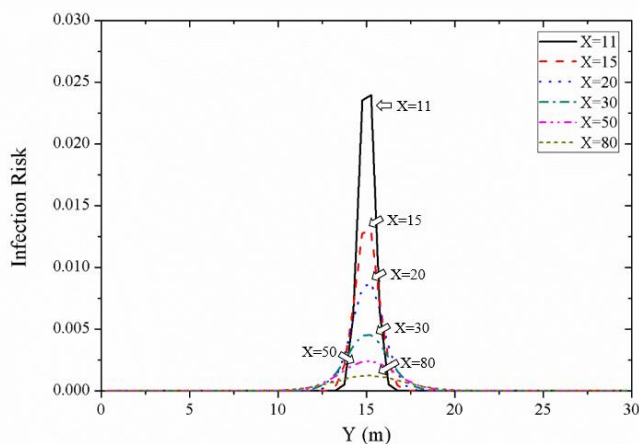


Fig. 6. Risk distribution in Y direction for different X location.

distribution function for each case. The fitting results are shown in Fig. 7.

As shown in Fig. 7, the distribution characteristic of these parameters meet the distribution characteristics of exponential distribution. So the distribution parameters can be quantitatively represented by the exponential distribution function, as follows:

$$\sigma(x) = a_{\sigma} e^{b_{\sigma}(x-X_0)} + d_{\sigma} \quad (4)$$

$$A(x) = a_A e^{b_A(x-X_0)}$$

Where a_{σ} , b_{σ} , d_{σ} , a_A and b_A are the characteristic parameters of the exponential distribution.

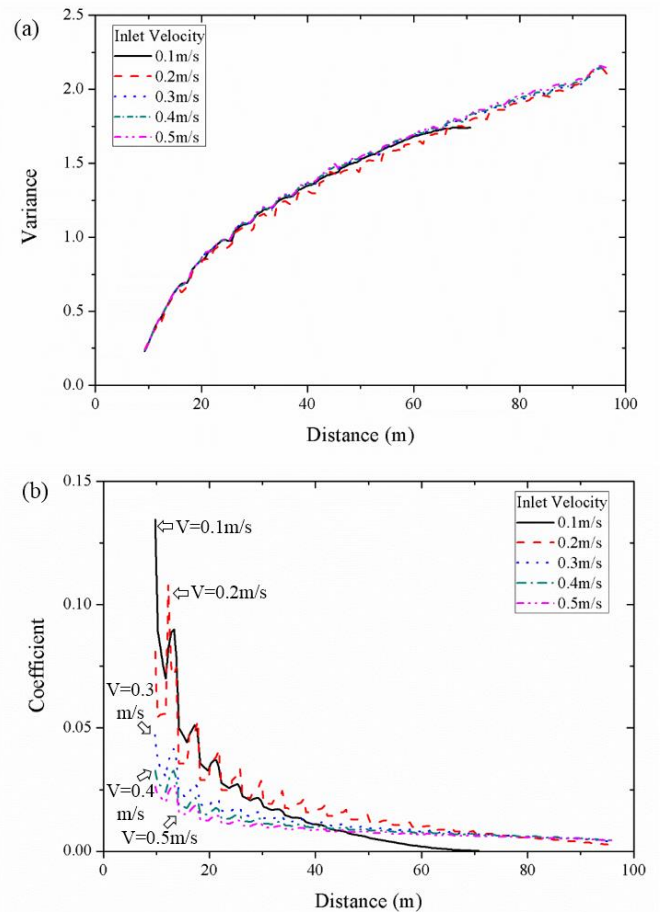


Fig. 7. Relationship between the characteristic parameters of risk distribution and the distance to the aerosol release source. (a) variance, (b) coefficient.

By using nonlinear least-square curve fitting analysis, the optimum values of the characteristic parameters can be obtained, as shown in Table III and IV. For the fitting results, the $p\text{-value} < 0.001$ and the adjusted $R^2\text{-values} > 0.99$. For multiple sources, the infection risk distribution can be calculated according to the risk distribution of each source, as follow:

$$P(x, t_0) = 1 - \prod_{i=1}^n (1 - P_i(x, t_0)) \quad (5)$$

TABLE III
FITTING RESULTS OF VARIANCE.

Average airflow velocity (m/s)	a_σ	b_σ	d_σ
0.1	1.9719	-2.2482	-0.0329
0.2	2.4344	-2.4599	-0.0194
0.3	2.3115	-2.3936	-0.0230
0.4	2.3293	-2.4150	-0.0228
0.5	2.3641	-2.4436	-0.0223

TABLE IV
FITTING RESULTS OF COEFFICIENT.

Average airflow velocity (m/s)	a_A	b_A
0.1	0.2207	-0.0856
0.2	0.0947	-0.0432
0.3	0.0409	-0.0291
0.4	0.0290	-0.0235
0.5	0.0228	-0.0205

In summary, the infection risk in indoor environment can be approximately estimated according to the average airflow velocity in the environment. The risk distribution can be calculated by equation (3)~(5), and the parameters needed can be obtained from Table III~IV combining with the average airflow velocity. This method can be used for the risk assessment of larger indoor environment, in which the accurate CFD calculation is infeasible because it is computationally expensive and demands much more computing resources and computing time.

IV. CONCLUSIONS

This work investigated the aerosol transmission process and the risk distribution characteristics in larger indoor environment. The Eulerian-Lagrangian approach was adopted for the aerosol dynamics simulation. The results indicated that the aerosol transmission process is highly depended on the airflow motion and ventilation mode. The affected region is decided by the location of the aerosol release source and the average airflow velocity. The infection risk distribution is assessed by using the dose-response model. A risk estimation method for airborne infectious diseases is proposed based on the distribution characteristics of the infection risk. The characteristic parameters of the distribution function can be calculated according to the average airflow velocity. This method can be a good help for the risk assessment of larger indoor environment in undeveloped countries.

REFERENCES

[1] World Health Organization. The world health report. Switzerland: The WHO press, 2004, Statistical annex.

[2] M. R. Moser, T. R. Bender, H. S. Margolis, G. R. Noble, A. P. Kendal, and D. G. Ritter, "An outbreak of influenza aboard a commercial airliner", *Am. J. Hyg.*, vol. 110, pp. 1-6, July 1979.

[3] T. A. Kenyon, S. E. Valway, W. W. Ihle, I. M. Onorato, and K. G. Castro, "Transmission of multidrug-resistant mycobacterium tuberculosis during a long airplane flight", *N. Engl. J. Med.*, vol. 334, pp. 933-938, Apr. 1996.

[4] S. J. Olsen, H.-L. Chang, T. Y.-Y. Cheung, A. F.-Y. Tang, T. L. Fisk, S. P.-L. Ooi, et al., "Transmission of the severe acute respiratory syndrome on aircraft", *N. Engl. J. Med.*, vol. 349, pp. 2416-2422, Dec. 2003.

[5] A. Mangili and M. A. Gendreau, "Transmission of infectious diseases during commercial air travel", *Lancet*, vol. 365, pp. 989-996, Mar. 2005.

[6] S. Yin, G. N. Sze-To, and C. Y. H. Chao, "Retrospective analysis of multi-drug resistant tuberculosis outbreak during a flight using computational fluid dynamics and infection risk assessment", *Build. Environ.*, vol. 47, pp. 50-57, Jan. 2012.

[7] C. Y. H. Chao and M. P. Wan, "A study of the dispersion of expiratory aerosols in unidirectional downward and ceiling-return type airflows using a multiphase approach", *Indoor Air*, vol. 16, pp. 296-312, Aug. 2006.

[8] C. Y. H. Chao, M. P. Wan, and G. N. Sze To, "Transport and removal of expiratory droplets in hospital ward environment", *Aerosol Sci. Technol.*, vol. 42, pp. 377-394, May. 2008.

[9] M. P. Wan, G. N. S. To, C. Y. H. Chao, L. Fang, and A. Melikov, "Modeling the Fate of Expiratory Aerosols and the Associated Infection Risk in an Aircraft Cabin Environment", *Aerosol Sci. Technol.*, vol. 43, pp. 322-343, Feb. 2009.

[10] J. Wang and T.-T. Chow, "Numerical investigation of influence of human walking on dispersion and deposition of expiratory droplets in airborne infection isolation room", *Build. Environ.*, vol. 46, pp. 1993-2002, Oct. 2011.

[11] Z. Q. Thai, W. Zhang, Z. Zhang, and Q. Y. Chen, "Evaluation of various turbulence models in predicting airflow and turbulence in enclosed environments by CFD: part 1 - Summary of prevalent turbulence models", *Hvac&r. Res.*, vol. 13, pp. 853-870, Nov. 2007.

[12] Z. Zhang, Z. Q. Zhai, W. Zhang, and Q. Y. Chen, "Evaluation of various turbulence models in predicting airflow and turbulence in enclosed environments by CFD: Part 2-comparison with experimental data from literature", *Hvac&r. Res.*, vol. 13, pp. 871-886, Nov. 2007.

[13] C. Y. H. Chao, M. P. Wan, L. Morawska, G. R. Johnson, Z. D. Ristovski, M. Hargreaves, et al., "Characterization of expiration air jets and droplet size distributions immediately at the mouth opening", *J. Aerosol. Sci.*, vol. 40, pp. 122-133, Feb. 2009.

[14] J. P. Duguid, "The size and the duration of air-carriage of respiratory droplets and droplet-nuclei", *J. Hyg.*, vol. 44, pp. 471-479, 1946. 1946.

[15] M. Nicas, W. W. Nazaroff, and A. Hubbard, "Toward understanding the risk of secondary airborne infection: Emission of respirable pathogens", *J. Occup. Env. Hyg.*, vol. 2, pp. 143-154, Mar. 2005.

[16] G. N. Sze To and C. Y. H. Chao, "Review and comparison between the Wells-Riley and dose-response approaches to risk assessment of infectious respiratory diseases", *Indoor Air*, vol. 20, pp. 2-16, Feb. 2010.

[17] D. H. Bennett, T. E. McKone, J. S. Evans, W. W. Nazaroff, M. D. Margni, O. Jolliet, et al., "Defining intake fraction", *Environ. Sci. Technol.*, vol. 36, pp. 207-216, May 2002.

[18] G. N. Sze To, M. P. Wan, C. Y. H. Chao, F. Wei, S. C. T. Yu, and J. K. C. Kwan, "A methodology for estimating airborne virus exposures in indoor environments using the spatial distribution of expiratory aerosols and virus viability characteristics", *Indoor Air*, vol. 18, pp. 425-438, Oct. 2008.

[19] A. C. Sims, S. E. Burkett, B. Yount, and R. J. Pickles, "SARS-CoV replication and pathogenesis in an in vitro model of the human conducting airway epithelium", *Virus Res.*, vol. 133, pp. 33-44, Apr. 2008.

[20] W. Nyka, "Studies on the infective particle in airborne tuberculosis. I. Observations in mice infected with a bovine strain of m. tuberculosis.", *Am. Rev. Respir. Dis.*, vol. 1, pp. 33-39, Jan. 1962.

[21] W. C. Hinds. Aerosol Technology. New York: John Wiley & Sons, Inc.; 1999. ch. 11.

[22] R. G. Loudon and L. C. Brown, "Cough Frequency in Patients with Respiratory Disease", *Am. Rev. Respir. Dis.*, vol. 96, pp. 1137-1143, Dec. 1967.